Comparison Between Ring and Radial Configurations of the University of Trieste Campus MV Distribution Grid

Massimiliano Chiandone, Stefano Quaia, Giorgio Sulligoi, Andrea Vicenzutti

***Abstract*—Distribution systems are being pushed towards smarter architectures, management strategies, and controls. To develop new platforms and algorithms for distribution systems management, the University of Trieste is using its medium voltage MW-scale ring distribution system as a demonstrator. In addition to the installation of a real-time monitoring system, power system studies and analyses are required. The paper presents and compares some results concerning the power system operation in both closed (normal operation) and open (post fault operation) configurations, where the latter are identified by means of a quantitative dependability analysis. In particular, the voltage profile, the currents, and the losses in the system are studied, evaluating the impact of faults capable of opening the ring.**

***Index Terms*- smart grid, ring distribution, power system monitoring, dependability analysis, power system simulation**

I. Introduction

The electric power distribution systems are transforming due to the increasing number of prosumers, energy storage systems, and users using large amounts of power electronics converters [1]. To correctly integrate these new elements, distribution systems must evolve, exploiting new architectures, management strategies, and controls. The first step towards smarter distribution systems is an increase in automation. Such direction already received a first strong push due to the incentivizing regulation of power quality introduced in Italy in 2000, as an effect of the electricity market liberalization process. However, further updates are required to shift from conventional MV ac distribution systems to smart grids. In this context, several projects focused on the MV ac distribution network automation have been developed [2] [3]. University of Trieste is working towards improving the distribution system in its main campus, to use it as a demonstrator for future smart grids. At present, a real-time monitoring system is being installed on the campus power system MV section [4] [5].

The MV distribution grid of the University of Trieste main campus has a ring topology at MW-scale, which makes it significant as a stepping stone (both in topology and power level) between the most common kW-scale demonstrators with radial topology, and experiments made on city/region-wide distribution systems. A ring topology enables a higher supply reliability level that a radial one, also providing lower voltage fluctuation at consumer's terminals [6]. This is due to the presence of two feeders, lying on different paths, supplying each secondary distribution substation. This also makes it possible to use a ring topology demonstrator to test some of the peculiarities of meshed systems, while a radial test system cannot do the same. Ring distribution systems are used primarily in the United Kingdom, where they were developed, and to a lesser extent in Ireland and in some other countries where the UK had a strong influence. Conversely, the use of a MV ring is an unusual peculiarity in Italy, thus making the availability of such an infrastructure a strength point for performing research on smart grids.

The increase in the campus distribution system smartness is aimed at supplementing the known ring distribution advantages with measurement and control devices. The latter will enable the optimal management of the ring, exploiting its specificity to support all the future electrical devices that can be installed in the campus (e.g., energy storage systems or distributed generation). However, several tests and studies are still required to define such management system. Along with the measurement infrastructure, simulations in different power system configurations are required. Following such needs, this paper presents and compares some preliminary results concerning the power system operation in both closed (i.e., normal operation) and open (i.e., post fault operation) configurations. The case study open ring configurations are determined through a dependability analysis [7], and then a comparison is made with closed ring operation focusing on voltage profiles, current in lines, and power losses.

In this paper, Section II presents the campus MV power system and its mathematical model. Section III briefly describes the measurement system that is being installed. Section IV presents the dependability analysis. The results of the simulations are shown and discussed in Section V. Finally, Conclusions are given in the last Section.

II. University of Trieste campus MV grid and mathematical model

The University of Trieste, located in the north-east of Italy, is divided in different campuses, depending on the specific degrees and masters offered to the students. Figure 1 shows the layout of the main campus. It is supplied with a dual feeder 27.5 kV delivery by the local distribution system operator (DSO), whose point of common coupling (PCC) is located in the C3 building (orange square in Figure 1). The primary substation of C3 building includes two redundant 27.5/3 kV transformers always connected in parallel, which supply the different buildings of the campus through a ring power grid (black lines in Figure 1). The latter works at 3 kV, and passes through each of the ten buildings' substations (green squares in Figure 1), where the supply for the local loads is achieved by means of one or more 3/0.4 kV transformers. Figure 2 provides an easy-to-understand representation of the campus ring power grid. The figure includes also substation B, which has been added after the ring construction and thus is directly supplied at 27.5 kV from the primary substation. The buildings MV/LV substations use the base architecture illustrated in Figure 3, with some differences depending on the number of installed transformers. Their rating is depicted in Table I, together with the number of the bus identifying the specific substation in the mathematical model used for the simulations. The cables, installed on cableways in dedicated service tunnels, have the ratings shown in Table II (worst case coefficients used for the current ratings calculation: ambient temperature 40° C – coeff. 0.91, 3 vertical racks and 3 cables in contact – coeff. 0.74) and the lengths reported in Table III. Finally, the transformers parameters are depicted in Table IV, in terms of short circuit voltage (V_{sc}), power (P_{sc}), reactance (x_{sc}) and resistance (r_{sc}), with the last two calculated using the power of each machine as the base for the *per unit* values.

The MV power distribution system of the campus has been modeled using pandapower, an open-source tool for power system modeling, analysis, and optimization based on Python language [8]. Figure 4 shows the one-line diagram of the model representing the overall MV distribution system of the campus, from the user side of the DSO delivery point to the main LV switchboards of the buildings. The model includes cable lines, transformers, and loads. The latter, represented as aggregated loads following each building's LV power distribution lines, are modeled using the data coming from the existing measurement system installed on the LV side of each building substation. The campus grid model allows to evaluate power flow, voltage profiles, currents and power losses, as well as testing different operating conditions for the system.

III. REAL-TIME MONITORING SYSTEM

A monitoring system is installed on the LV side of each substation and is used for local energy management purposes. A new monitoring system, based on an open real-time HW/SW platform, is also being developed and installed for managing the MV ring. It takes advantage of a fiber-optic communication system, which connects all the substations with a ring architecture mimicking the power system one (the communication cables are laid near to the power ones). This communication infrastructure allows fast data exchange among all the substations, aimed at transmitting measurement data from each substation to the concentrator installed in substation C3. The architecture is made by a PC with an I/O digital-analogic conversion card, on which a real-time signal acquisition, conditioning, and transmission process runs.

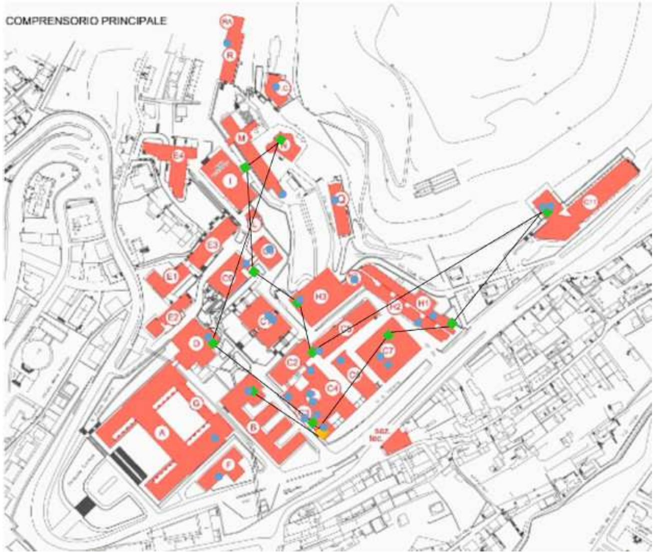

Figure 1. University of Trieste buildings layout [5]

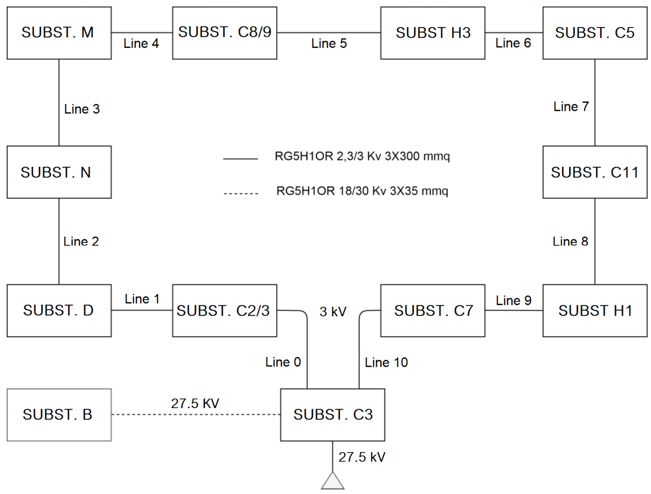

Figure 2. University of Trieste MVAC distribution grid topology

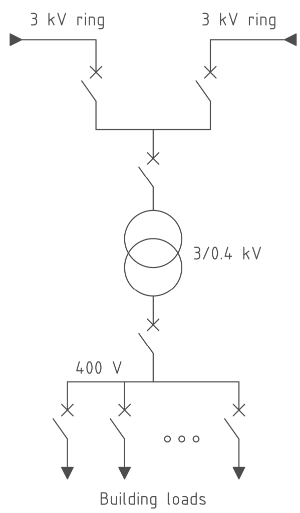

Figure 3. Buildings MV/LV substations architecture

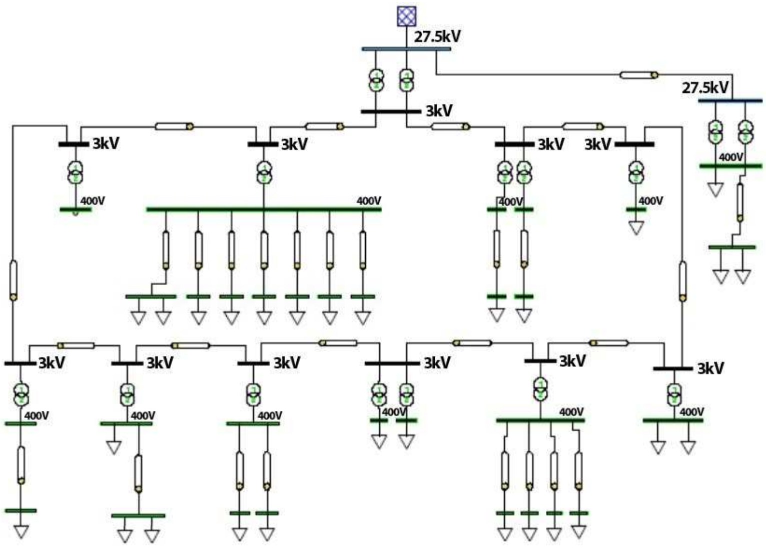

Figure 4. One-line diagram model of the campus MV grid [4]

TABLE I. UNIVERSITY OF TRIESTE SUBSTATIONS RATED POWER

Substation name	Rated power of substation transformers	Bus #
SUBSTATION C3	2x 1600 kVA (redundant)	1
SUBSTATION C2-3	630 kVA	2
SUBSTATION D	630 kVA	3
SUBSTATION N	400 kVA	4
SUBSTATION M	400 kVA	5
SUBSTATION C8-9	250 kVA	6
SUBSTATION H3	2x 400 kVA (used both only in summer)	7
SUBSTATION C5	1000 kVA	8
SUBSTATION C11	2x 1000 kVA (only one used)	9
SUBSTATION H1	1x 800 kVA – 1x 250 kVA (not used)	10
SUBSTATION C7	1x 315 kVA – 1x 250 kVA	11
SUBSTATION B	2x 1000kVA	/

TABLE II. DISTRIBUTION SYSTEM MV CABLES RATINGS

Cable type	Voltage rating [kV]	Cond. # and section [mm^2]	Current rating [A]	Resistance @ 90° C [Ω/km]	Reactance [Ω/km]	Capacity [μF/km]
RG5H1OR	2,3/3	3x300	427	0.0807	0.072	0.75
RG5H1OR	18/30	3x35	162	0.669	0.14	0.14

TABLE III. DISTRIBUTION SYSTEM MV CABLE LENGTHS

Line	Line #	Length [m]
C3 - B	-	131
C3 – C7	10	162
C7 – H1	9	133
H1 – C11	8	250
C11 – C5	7	360
C5 – H3	6	66
H3 – C8/9	5	68
C8/9 – M	4	193
M – N	3	56
N – D	2	260
D – C2/3	1	252
C2/3 – C3	0	5

TABLE IV. SUBSTATION TRANSFORMERS PARAMETERS

Power [kVA]	V_{sc} [%]	P_{sc} [W]	X_{sc} [p.u.]	R_{sc} [p.u.]
250	6	3500	0.059	0.014
315	6	4200	0.059	0.013
400	6	4900	0.059	0.012
630	6	7300	0.059	0.012
800	6	9000	0.059	0.011
1000	6	10000	0.059	0.01
1600	6	14500	0.059	0.009

Each device can monitor up to 9 currents and 3 voltages with a 600 Hz sampling frequency, convert them individually in Park vectors, and finally transmit every 10 ms the resulting data over the communication system to a dedicated machine for elaboration and storage. The sampling is made through 12 bit analog-to-digital converters, with a measuring range focused around the rated voltage (virtually increasing the resolution, at the expense of the overall measurement range). Such capability enables to remotely monitor the MV ring distribution system, by acquiring, elaborating, and storing data concerning its power quality (current and voltages waveforms, frequency, active and reactive power, and other indexes). The open real-time HW/SW architecture is also ready for sending commands to the remote devices, thus enabling the future upgrade of the MV ring power system towards a smart grid.

IV. DEPENDABILITY ANALYSIS OF THE CAMPUS MV GRID

The campus MV ring normally operates in closed ring configuration. However, faults can force the system in open ring configuration, with a direct impact on the system power quality, until a repair activity is completed. To identify the most significant configurations to be simulated using the above-described mathematical model, a quantitative Failure Tree Analysis (FTA) [7, 9, 10] has been performed. The top event used for the FTA is the open ring configuration for the 3 kV ring distribution system, while the components considered in the study are circuit breakers, switchgears,

TABLE V. FAILURE MODELS PARAMETERS

Component	Failure rate [failures/y]	MTTR [h]
Switchgear	$1.917*10^{-3}$	17.3
Circuit Breaker	$3.6*10^{-3}$	109
Cable terminations	$0.303*10^{-3}$	25
Cable	$6.13*10^{-3}$ for 1000 ft	96.8

TABLE VI. QUANTITATIVE FTA RESULTS

Line	Failure frequency [failures/y]	Number of expected failures in 20 years	Total down time in 20 years [h]
Open ring	0.143	2.86	253.2
7	0.015	0.301	30
2	0.013	0.261	26.1
1	0.0129	0.257	25.8
8	0.0128	0.257	25.7
4	0.017	0.234	23.5
10	0.0111	0.221	22.3
9	0.0105	0.210	21.2
5	0.00917	0.184	18.7
6	0.00913	0.183	18.6
3	0.00839	0.179	18.2
0	0.00791	0.158	16.2

TABLE VII. SUBSTATIONS LOAD FROM MEASUREMENTS ON LV SIDE

Substation name	Active power [kW]	Reactive power [kvar]
SUBSTATION C2-3	218	88
SUBSTATION D	120	60
SUBSTATION N	101	43.2
SUBSTATION M	152.1	67
SUBSTATION C8-9	16.1	0.76
SUBSTATION H3	108	45
SUBSTATION C5	78	20.2
SUBSTATION C11	320	150
SUBSTATION H1	23	9
SUBSTATION C7	14	0.66
Tot	**1150.2**	**483.8**

cables, and cable terminations. Table V shows the dependability data used for the quantitative study, expressed in terms of failure frequency and Mean-Time-To-Repair (MTTR), using the "industry average" values of IEEE Std. 493-2007 [11]. The cable failure rate is expressed in per unit length values (failure rate for a 1000 ft cable length), thus each cable in the MV network has its specific failure rate, depending on its length (Table III).

The results of the quantitative FTA are shown in Table VI, in descending order of failure frequency. The timeframe used for the number of expected failures and total downtime calculations is 20 years. The "open ring" item refers to the cumulative results of all the possible single line opening events (i.e., the opening of the ring at any point). As it is evident from the results, an event leading to the ring opening is very rare (less than 3 events in 20 years), and leads to an open ring operation time of just above 250 hours. Still, in open ring all the loads are kept supplied, and at least two faults are required for causing a disservice to the LV loads.

Given the results of the analysis, it has been decided to study the system behavior in the four most frequent open ring conditions: line 7, 2, 1, or 8 failed. The simulation results are presented and discussed in the next section of the paper.

V. SIMULATIONS

The results shown in this paper only concern the 3 kV ring section of the campus MV distribution system. Thus, substation B is excluded from the simulations, as it is directly supplied at 27.5 kV from the PCC located in substation C3. The simulations have been performed using as input data the measurements coming from the LV side measurement system and concerning a high load operating condition. The loads applied to each substation are depicted in Table VII. The total load is nearly 1250 kVA, with a global power factor of 0.92.

Different simulations have been performed, aiming to compare the operation of the closed ring and the four different open ring conditions individuated in Section IV. The comparison highlights the differences in voltage profiles, current loading of the ring cables, and active power losses.

The closed ring configuration presents a low voltage drop (Figure 5), which never exceeds 1.5% despite the high load condition chosen for the system. Regarding the currents, in closed ring operation they are well below the cable ampacity, as Figure 6 results and Table II current ratings clearly show.
The most frequent open ring operation follows a failure on line 7. This event causes a negligible effect on the bus voltages, as Figure 7 shows. This is due to the low current loading of such line, which causes small variations in the currents after the opening (Figure 8). The opening of line 2 has a more substantial effect on both voltages (Figure 9) and currents (Figure 10), being such line closer to the ring supply point. In particular, the maximum voltage drop rises above 3%, while the most loaded lines shift from one side of the ring to the other, although the maximum current value does not increase by much.

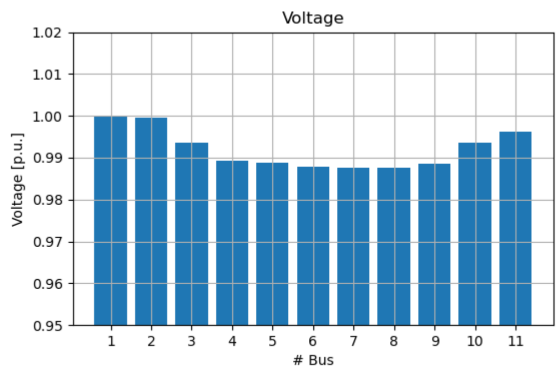

Figure 5. Voltage profile in per unit, closed ring configuration

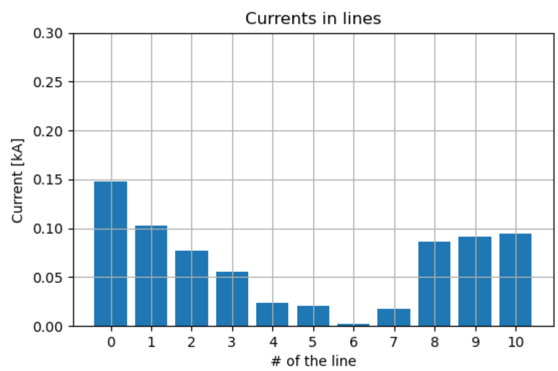

Figure 6. Current on the lines, closed ring configuration

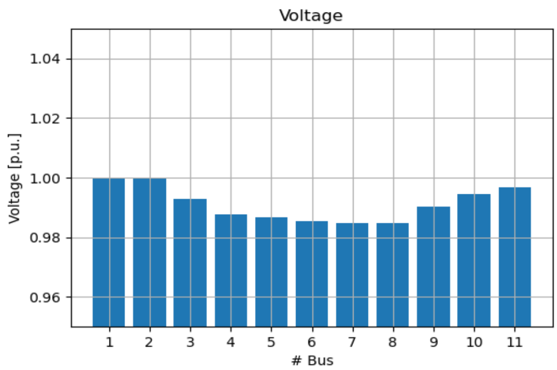

Figure 7. Voltage profile in per unit, ring open on line 7

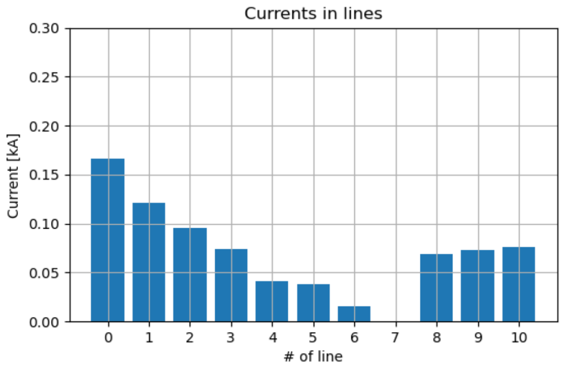

Figure 8. Current on the lines, ring open on line 7

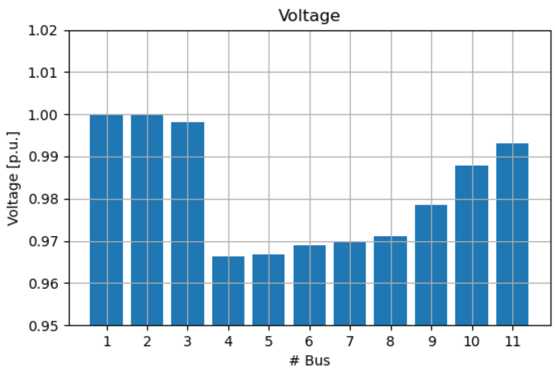

Figure 9. Voltage profile in per unit, ring open on line 2

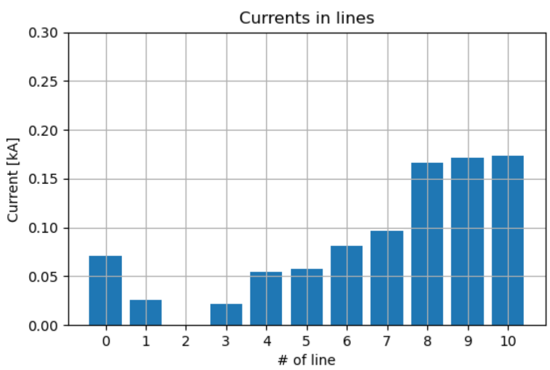

Figure 10. Current on the lines, ring open on line 2

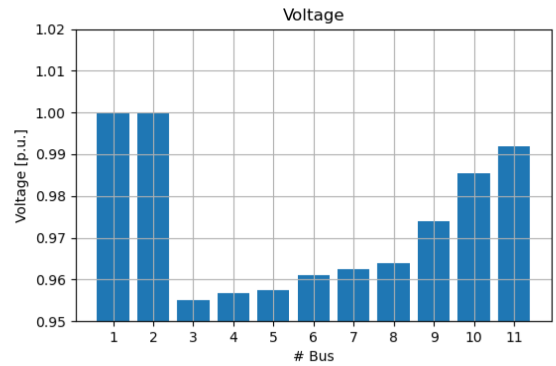

Figure 11. Voltage profile in per unit, ring open on line 1

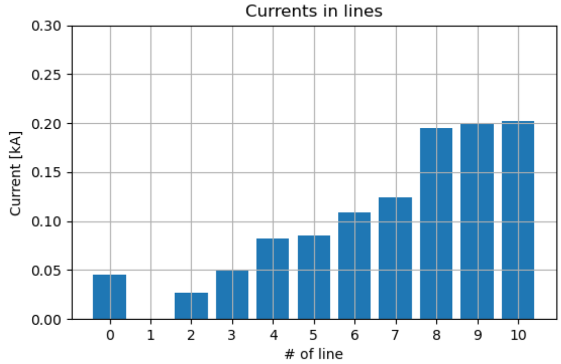

Figure 12. Current on the lines, ring open on line 1

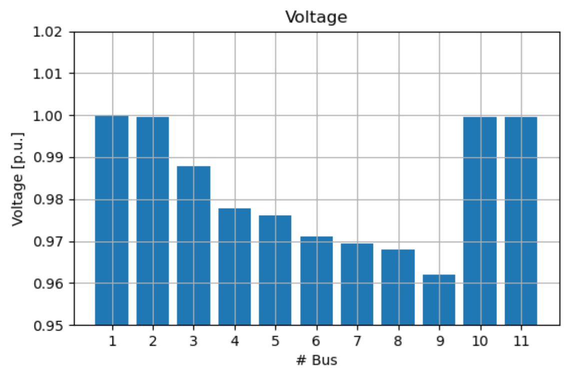

Figure 13. Voltage profile in per unit, ring open on line 8

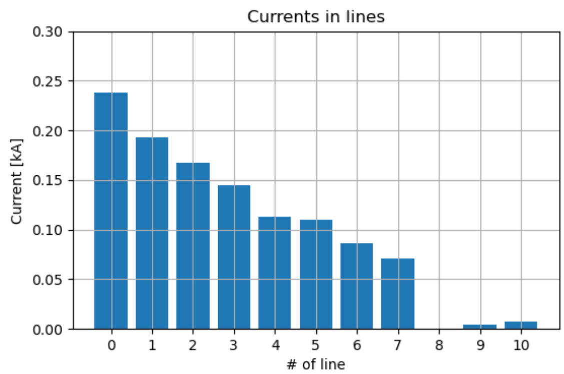

Figure 14. Current on the lines, ring open on line 8

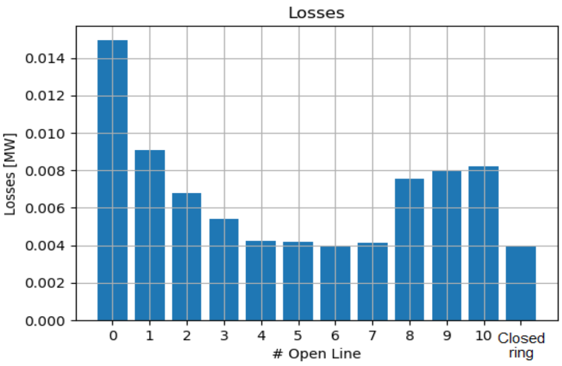

Figure 15. Active power losses with ring closed and open at a single bus

The third most frequent failure concerns line 1, which has similar effects to the previous case due to its location (refer to Figures 11 and 12). However, this configuration leads to the highest voltage drop of all the simulated ones, which exceeds 4% on buses 3, 4 and 5 (about three times the maximum voltage drop in the closed ring). The low voltage on Substation D, N, and M (buses 3, 4, and 5) may be critical for the loads. Indeed, being the results referred to the MV side of the substations, the voltage drop at the LV loads will be higher due to the impedances of the MV/LV transformers and the LV distribution cables. The fourth most frequent open ring condition follows line 8 opening. The results are similar to line 2 opening in terms of both voltages (Figure 13) and currents (Figure 14), although mirrored. This operating condition leads to the highest current loading in the first lines, which increases by about 60% in line 0 in respect to the closed ring configuration. The resulting current is still lower than the cable ampacity, making it possible to work in this post fault condition until the fault is repaired with no adverse issues for the system. Comparing the voltage and currents results in open ring configurations, the following can be highlighted. The highest current loading occurs when line 8 is opened, and the highest voltage drop occurs when line 1 is opened. This is due to non-uniform load distribution on the ring, where Subst. C11 and H1 (connected by line 8) are among the least loaded ones, and Substation C2/3 and D (connected by line 1) are among the most loaded ones.

Finally, Figure 15 shows the active power losses in the MV system, considering all the components from the PCC to the output of the MV/LV transformers in the buildings substations. The losses have been calculated in both the closed ring configuration and in all the possible open ring ones. The highest losses are with line 0 opened, and reach up to 3.75 times the closed ring losses. This happens because line 0 is the most loaded one, since it is the closest line to the most loaded substations. However, a failure on line 0 is also the least frequent among all the considered ones. Conversely, the most frequent event, which is line 7 opening, has almost no effect on the losses, since this line is lightly loaded. Of course, the economic impact of the power losses depends not only on their amount, but also on their duration (i.e., the impact depends on the energy losses). By using the total downtime (Table VI) and the power losses (Figure 15) for each open ring configuration, it is possible to evaluate the energy lost in 20 years of system operation in both normal and faulted condition. The lost energy is equal to nearly 702 MWh, where the impact of the open ring operation amounts to less than 0.1%. This is because open ring operation is only temporary. Thus, no appreciable economic impact can be highlighted if the closed ring configuration is the standard one, while it may become significant if the ring is operated in open configuration for long periods of time [6].

CONCLUSIONS

This paper compares and discusses results of mathematical simulations concerning the University of Trieste MV ring distribution system. The system is studied in both closed (normal operation) and open (post fault operation) ring configurations, where the interruption points for the latter are defined by identifying the most probable fault events through a quantitative dependability analysis. The comparison is made in terms of voltage profiles on the ring, currents on the lines, and total active power losses.

As expected, the closed ring configuration provides the lowest voltage drops and power losses, as well as the most uniform current distribution. Conversely, opening the ring in different locations (due to faults) may lead to excessive voltage drop at some substation terminals, as well as to considerably increased currents in some lines (still remaining below cables ampacity). The power losses can also increase significantly, but the economic impact on the system operation is negligible thanks to the temporary nature of such condition.

REFERENCES

[1] E. Lightner, "Evolution of distribution, impacts on grid planning and operations", in *IEEE Power and Energy Magazine*, vol. 18, no. 1, pp 92 –96, Jan.-Feb. 2020.

[2] H. B. Cetinkaya, S. Kucuk, M. Unaldi and G. B. Gokce, "A case study of a successful industrial microgrid operation," *2017 4th International Conference on Electrical and Electronic Engineering (ICEEE)*, Ankara, Turkey, 2017, pp. 95-98.

[3] P. Marino, G. Rubino, L. Rubino, C. Capasso, O. Veneri and I. Motori, "A case study of a DC-microgrid for the smart integration of renewable sources with the urban electric mobility," *2018 International Symposium on Power Electronics, Electrical Drives, Automation and Motion (SPEEDAM)*, Amalfi, Italy, 2018, pp. 544-549.

[4] M. Chiandone, M. D.Feste, D. Bosich and G. Sulligoi, "Real-time monitoring and control system for Trieste University Campus electrical distribution grid," *2019 IEEE Milan PowerTech*, pp. 1-5

[5] M. D. Feste, M. Chiandone, D. Bosich and G. Sulligoi, "The Control and Monitoring System on a Medium Voltage AC Distribution Grid: Device Implementation and Calibration Procedure," *2021 IEEE 15th International Conference on Compatibility, Power Electronics and Power Engineering (CPE-POWERENG)*, 2021, pp. 1-6

[6] R. J. W. de Groot, J. Morren and J. G. Slootweg, "Investigation of grid loss reduction under closed-ring operation of MV distribution grids," *IEEE PES General Meeting | Conference & Exposition*, 2014, pp. 1-5

[7] A. Vicenzutti, R. Menis and G. Sulligoi, "All-Electric Ship-Integrated Power Systems: Dependable Design Based on Fault Tree Analysis and Dynamic Modeling," in *IEEE Transactions on Transportation Electrification*, vol. 5, no. 3, pp. 812-827, Sept. 2019

[8] L. Thurner et al., "Pandapower—An Open-Source Python Tool for Convenient Modeling, Analysis, and Optimization of Electric Power Systems," in *IEEE Transactions on Power Systems*, vol. 33, no. 6, pp. 6510-6521, Nov. 2018

[9] S. Kabir, "An overview of fault tree analysis and its application in model based dependability analysis", *Expert Syst. Appl.*, vol. 77, pp. 114-135, Jul. 2017.

[10] IEC, 61025, "Fault Tree Analysis (FTA)", Dec. 2006.

[11] IEEE, 493-2007, "IEEE Recommended Practice for the Design of Reliable Industrial and Commercial Power Systems", Jun. 2007.